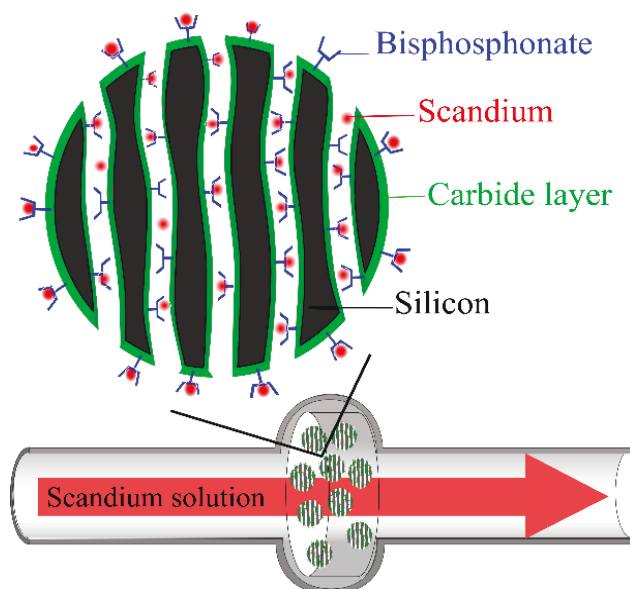Rinez Thapa, Tuomo Nissinen, Petri Turhanen, Juha Määttä, Jouko Vepsäläinen, Vesa-Pekka Lehto, Joakim Riikonen

Bisphosphonate modified mesoporous silicon for scandium adsorption

Working title: Bisphosphonate functionalized on carbonized mesoporous silicon for scandium adsorption.

Graphical abstract

Abstract

Bisphosphonate molecules were grafted on thermally carbonized surfaces of mesoporous silicon. The nanostructured material retained high surface area (220 m^2/g), pore volume (0.56 cm^3/g) and pore diameter of 10 nm while the functionalized molecules were 2 % w/w. The adsorption isotherm of scandium followed Langmuir model resulting maximum capacities of 26 µmol/g at pH 1 and 51 µmol/g at pH 3. Efficiency of this material to adsorb/desorb scandium was examined in a simple flow-through setup. The adsorbent exhibited remarkable selectivity towards scandium measured by a separation factor, which was 3-fold superior to a commercialized ion exchange resin Dowex 50WX8, examined in an equimolar mixture of Sc, Fe, Al, Cu and Zn at pH 1. Crucially, the hybrid material proved to be highly stable and reusable upto 50 adsorption/desorption cycles of scandium.

1. **Introduction**

Scandium (Sc) is an essential metal in the development of high-tech materials and modern technology. It is mainly used as an effective alloying element (0.2 – 0.6 wt. % Sc) with aluminum. The Sc-Al alloys (stronger, lighter and resistant to corrosion) are used in aerospace industry, transportation and sports equipment.[1] Utilization of Sc is growing in solid oxide fuel cells because of high oxygen ion conductivity of Sc_2O_3-stabilized-ZrO_2 solid electrolytes even at lower temperatures.[2] Recently, Sc has been used to enhance the piezoelectric response in aluminum nitride alloys.[3] Other applications are in ceramics, high intensity metal halide lamps and lasers.[4]

Regardless of the numerous applications, extensive use of Sc has not been feasible due to its scarcity and high price. For instance, current price of Sc_2O_3 with 99.99 % purity is 4600 US$/kg while the Sc ingot costs 132000 US$/kg.[4] Sc is expensive because the metallurgical processes involved in its purification and recovery is very difficult and time consuming. Exploitable ores

of Sc (e.g. thortvitite) are rare; however, Sc often co-exists in ores of other minerals but its quantity is highly dispersed and occurs in low concentrations.[5] Exploitation of these ores containing trace Sc is not economically viable. Therefore, Sc is usually recovered as a by-product from the waste residues and tailings of other metal mining such as uranium-leached liquors, titanium pigment production wastewaters, tungsten refinery and bauxite residues.[6]

Conventional hydrometallurgical processes used in the recovery such as precipitation and solvent extraction have major drawbacks. The precipitation method yields poor Sc purity due to co-precipitation of impurity metals present in larger quantities.[5,6] Solvent extraction is principally operated in large-scale and requires treatments with a large volume of hazardous organic solvents that lead to potential toxic emissions into the environment.[7] Also economically, the methods are not convenient for low content Sc due to the high acid consumption as well as the complications associated to reuse the extractant.[8]

As a greener alternative, adsorption technology has the potential to extract Sc more efficiently in terms of low operating cost, easy to use and reusability. Fundamental requirement here is that the adsorbent material is capable to reversibly adsorb and desorb Sc ions and substantially in repeated cycles without reduction in the performance. Moreover, the efficacy of the material is determined by its ability to selectively capture Sc from the metal impurities. Hence, physiochemical characteristics of the adsorbent is the key foundation to succeed profitable Sc extraction and its commercialization.

Commercially available adsorbents such as ion exchange resins mainly suffer from aggregation and fouling problems due to the swelling of its polymeric structure during adsorption-desorption processes, which eventually leads to deterioration of the material.[9,10] To overcome these issues, chemical anchoring of metal binding molecules onto a rigid support is promising technique in the state-of-the-art. In particular, mesoporous silica have been widely used because of their high surface areas offering high degree of functionalization.[8] But the stability of the silica-based material is yet limited in highly acidic conditions due to the dissolution of extremely thin pore walls.[8,11] Besides, the reusability of the hybrid materials are rarely reported for more than 10 cycles and is usually done in batch setup, which is a tedious task in large scale operation.[12-17]

Flow through setup is simpler technique to adsorb/desorb metals in continuous process, in which the volume and speed of the feed solution are easily controlled. The hybrid materials can be conveniently packed in column where the metal solution can swiftly flow through because of high permeability assisted by the parallel pores in the material.

Nevertheless, not only the mesoporous silica support but also the functionalized molecules must be robust to sustain the reusability of the adsorbent. Bisphosphonates consisting O=P–C–P=O structure are stable molecules that have been demonstrated to collect several metal cations from mining process waters.[18] In our earlier research, bisphosphonate molecules with terminal alkene were directly grafted on thermally carbonized surfaces of mesoporous silicon. The synthesized material showed exceptional stability in highly acidic/basic solutions.[JR paper] In this study, we investigate the adsorption mechanisms alongside the selectivity towards Sc, and the chemical stability and reusability of this material up to 50 adsorption/desorption cycles. Further, we demonstrate a flow through setup where the material is used as filters in columns

to extract scandium efficiently. The obtained results were compared to a commercialized ion exchange resin Dowex 50WX8 operated in analogous experimental conditions.

2. Experimental section

2.1 Materials, chemicals and standard solutions

Hydrofluoric acid (HF 38–40 %, Merck), ethanol (EtOH 99.5 %, Altia Oy) and silicon wafers (Okmetic Oyj) were used for preparation of porous silicon (PSi). Bisphosphonate molecule (*Tetrakis(trimethylsilyl) 1-(trimethylsilyloxy)undec-10-ene-1, 1-diylbisphosphonate)* was synthesized and characterized as reported elsewhere.[JR paper] Standard solution of Sc (1000 mg/L in 1 wt % HNO_3, AAS standard) and the ion-exchange resin, Dowex 50WX8 (hydrogen form, 100 – 200 mesh) were purchased from Sigma, Finland. The resin is a strong cation exchanger containing sulfonic acid (SO_3H) functional groups. Metal standards (1000 mg/L) of $AlCl_3$, $FeCl_3$, $CuCl_2$ and $ZnCl_2$ were all Titrisol standards purchased from Merck, Finland. Milli-Q water was used throughout the experiments.

2.2 Synthesis of porous silicon (PSi). Silicon wafers with resistivity values of 0.01–0.02 Ωcm were electrochemically etched in 1:1 HF/EtOH mixture applying current density of 30 mA/cm^2 for 40 min. PSi films were detached from the wafers with lift-off current pulses of 160 (1 sec) and 255 mA/cm^2 (2 sec) with 1 sec pause between the pulses. The films were then dried for 1 h at 65 °C. The dry PSi films were first hand ground into coarse particles and later milled (100 rpm, 3 mins) in a planetary ball mill (Fritsch Pulverisette 7). The particles were then sieved into 25–75 µm size fraction.

2.3 Thermal carbonization of PSi. The PSi micro particles were immersed in 1:1 HF/EtOH solution for 10 min. Supernatant was discarded and the sample was dried for 45 min at 65 °C. The dry PSi powder was transferred into a quartz tube and flushed with N_2 for 30 min at 1 L/min. Acetylene gas at 1 L/min was infused first for 15 min at room temperature (RT) followed by treatment for 14 min 30 sec at 500 °C in preheated tube oven. After 30 sec of only N_2 at 500 °C, the quartz tube/sample was taken out from the tube oven and the sample was cooled at RT for 30 min under N_2. At the room temperature, the acetylene flow was resumed for 9 min 40 sec. After 20 sec, the sample was heated at 820 °C for 10 minutes under N_2 in the tube oven. The manufactured thermally carbonized particles (TCPSi) were cooled at RT for 40 min under N_2 atmosphere.

2.4 Synthesis of BP-TCPSi. The BP molecule was conjugated on TCPSi particles by mixing 1:2 mass ratio of BP:TCPSi under N_2 protection. Before the mixing, BP was formerly degassed in mesitylene solution using N_2 gas for 20 min. The mesitylene solution containing the BP was transferred into the quartz tube and mixed with the TCPSi particles. The quartz tube was sealed with a Teflon stopper and the sample was incubated at 120 °C under N_2 atmosphere. After 19 h, the BP-TCPSi particles and mesitylene solution was poured into a beaker. The unbound BP molecule and mesitylene supernatant was discarded by washing the particles thrice with 40 mL MeOH. The particles were washed with 100 mL MeOH in suction filtration (polypropylene PP filter, 10 µm pore size) and dried at 65 °C for 1 h. Similarly prepared TCPSi particles incubated in mesitylene without BP was used as reference sample.

2.5 Material characterization and instrumentation

The median particle size of TCPSi and BP-TCPSi samples was measured by Mastersizer device (Mastersizer 2000, Malvern Instruments, UK) using EtOH as dispersant. The surface area, pore volume and pore diameter of the particles was determined by N_2 adsorption/desorption isotherms (Micromeritics Tristar III). Prior to the measurement, samples were degassed at +65 °C in vacuum (VacPrep 061, Micromeritics) for 1 h and then the sample chamber was filled with controlled increments of N_2 at temperature of 77 K (-196.15 °C).

The amount of BP grafted on TCPSi was measured by thermogravimetric analysis (TGA Q50, TA instruments). Samples were first equilibrated at 80 °C for 30 min and then heated to 700 °C at the rate of 20 °C/min under nitrogen flow (120 mL/min), and the mass loss was measured as a function of temperature. The BP content (% w/w) from BP-TCPSi sample was calculated by comparing the mass loss to unfunctionalized TCPSi sample.

Samples for scanning electron microscope (SEM, Zeiss Sigma HP VD) coupled with energy dispersive X-ray spectroscopy (EDS, ThermoScientific) were prepared by clueing the microparticles on top of standard aluminium stub with conducting carbon adhesive. 5.0 kV acceleration voltage was used with SE2 or InLens Detector for the images of the particles and the acceleration voltage was increased to 15.0 kV for EDS analysis.

2.6 Adsorption studies

2.6.1 Batch setup

Batch experiments were conducted in 15 mL centrifuge tubes by mixing 10 mg of the adsorbent material (TCPSi, BP-TCPSi or Dowex 50WX8) in 10 mL of Sc solution at desired concentration and pH. The pH of the metal solutions was adjusted with HNO_3 or NaOH.

Before contacting with the Sc solution, adsorbents were primed by mixing (for 1 h) in acidic media; the TCPSi or the BP-TCPSi particles in 10 ml of 5 M HCl whereas the Dowex 50WX8 resin in 10 ml of 0.125 M H_2SO_4, and washed three times with 10 mL Milli-Q water to obtain neutral pH. Subsequently, the Sc solution was contacted with adsorbent for a pre-determined time by mixing in an orbital shaker at shaking speed of 80 rpm. The adsorbent was separated from the suspension by centrifugation (6000 rpm, 1 min) and the supernatant aliquot was measured by inductively coupled plasma mass spectrometer, ICPMS (NexION 350D, Perkin Elmer). The adsorbed metal amounts (Q_e in µmol/g) was calculated using following equation.

$$Q_e = \frac{(C_o - C_e)V}{m} \times \frac{1000}{MW} \qquad (1)$$

Where, C_0 and C_e are the metal concentration (mg/L) before and after the adsorption respectively, m is the mass (mg) of adsorbent and 'V' is the volume (mL) of metal solution whereas MW represents the molecular weight (g/mol) of the metal ion.

2.6.2 Flow-through setup

Lab-scale flow through setup (supplementary Figure S1) consisted of a syringe pump (AL-1600, New Era Pump Systems Inc.), conventional 30 mL plastic syringes and glass columns (Omnifit® Labware, 2.5 cm × 0.3 cm i.d. volume capacity 0.2 mL). 20 mg of either the BP-TCPSi particles or the Dowex 50WX8 resin were packed inside the column supported onto polypropylene (PP) filter of 10-µm pore size. Unlike large rigid BP-TCPSi microparticles,

Dowex 50WX8 resin was viscous; it was not possible to pour the resin into the column. Therefore, the resin was first dispersed in water and then pushed into the column using a syringe. Priming was done by filtering 5 ml of the acidic solution mentioned above applying the flow rate of 0.2 mL/min. After that, adsorbents were washed with 10 mL water at 1 mL/min. Adsorption step was carried out by filtering 5 mL of the metal solution at 0.25 mL/min, whereas desorption with 15 mL of 1 M HNO_3 at 1.25 mL/min. After every adsorption or the desorption step, adsorbent was washed with water as described above. Duration for a complete cycle was 52 min. Desorbed metal amount (D_a in µmol/g) was calculated using following equation.

$$D_a = \frac{C_{des} \times V}{m} \times \frac{1000}{MW} \qquad (2)$$

Where, C_{des} is the metal concentration after desorption step.

3. Results and discussion

3.1 Characterization of BP-TCPSi

The median particle size of BP-TCPSi was 73.3 µm (particle size distribution shown in Figure S2). SEM results (Figure 1) revealed the irregular morphology of the microparticles (25 -75 µm) and pores openings on the surface of the BP-TCPSi particles. The N_2 sorption isotherms were typical type IV, showing hysteresis of mesoporous structure and the isotherm shape was unchanged after BP functionalization (Figure S3). The results from the gas adsorption are summarized in Table 1. The conjugation of BP molecules did not reduce the pore volume and pore diameter significantly therefore did not deter the pore openings and a considerable surface area (220 m^2/g) was preserved. The amount of BP grafted on TCPSi was quantified by TGA curves (Figure 2) and the mass loss calculated at 580 °C was 1.97 ± 0.03 % w/w equivalent to 59 ± 1 µmol BP per gram of the sample. The presence of BP on TCPSi was further confirmed from EDS analysis (Figure S4), where a clear phosphorous peak at 2.01 KeV was detected in the spectrum of BP-TCPSi sample but not in TCPSi sample.
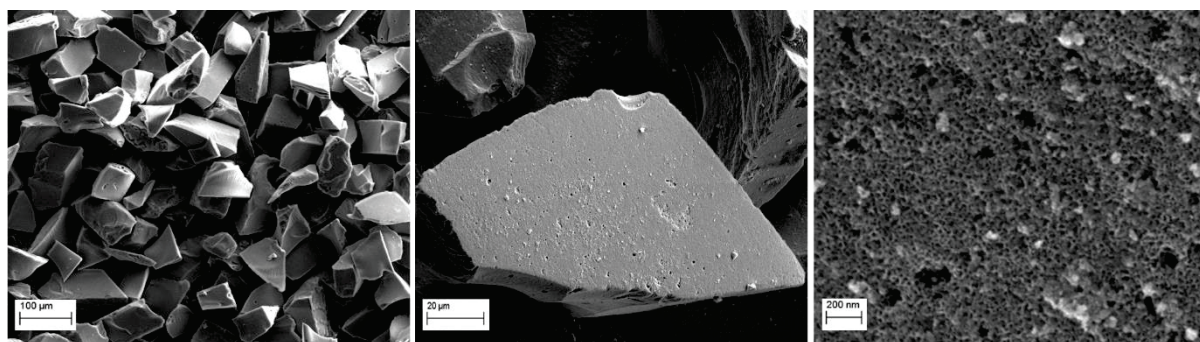

Figure 1. SEM results showing the morphology and porous structure of BP-TCPSi particles.

Table 1. Results from N_2 physisorption of TCPSi and BP-TCPSi samples (mean ± SD, *n*=3).

Materials	Surface area[a] (m²/g)	Pore volume[b] (cm³/g)	Pore diameter[c] (nm)
TCPSi	250 ± 3	0.65 ± 0.01	10.5 ± 0.1
BP-TCPSi	220 ± 2	0.56 ± 0.01	10.1 ± 0.1

a. BET surface area calculated from the isotherm.

b. Specific pore volume calculated from desorption isotherm at p/p0 = 0.9.

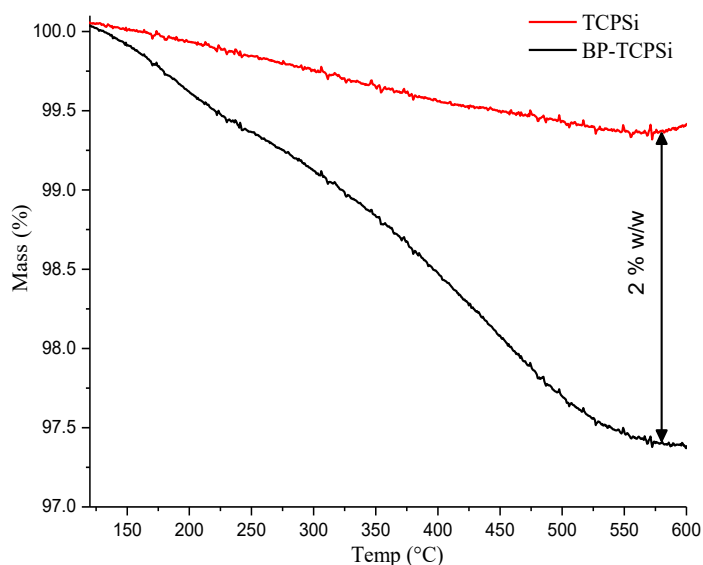*c.* Average pore diameter calculated by BJH theory using desorption branch of isotherm.

Figure 2. TGA curves of TCPSi and BP-TCPSi samples.

3.2 Adsorption studies

3.2.1 Batch setup

It was inferred that the extent of Sc adsorption depends upon the solution pH due exchange of protons in BP moeity with the metal ions. Deprotonation constant; pKa values of BP molecule (Figure 3) are pKa_1=1.0, pKa_2 = 2.5, pKa_3 = 6.7, pKa_4 =10.6 and pKa_5 =11.6.[19]
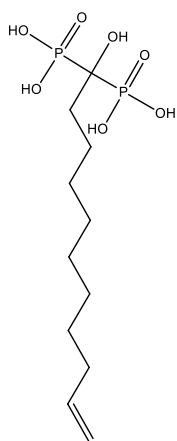
Figure 3. Chemical structure of bisphosphonate molecule grafted on the BP-TCPSi particles.

At pH $\geq$ pKa; deprotonation occurs. To avoid unspecific adsorption and the risk of Sc precipitation at pH >4[13,20,21], the adsorption studies were performed at pH 1 and pH 3. The studies were started with by examining the kinetics of the adsorption in order to find out the equilibrium time for the adsorption isotherm studies in batch type setup. This resulted equilibrium time of 4 h for pH 1 and 24 h for pH 3, determined from the starting of plateau in

adsorption curves (Figure S5). Adsorption was faster at pH 1 requiring only 10 min for 50 % adsorption while it took at least 1 h at pH 3. Based on the kinetics, 24 h time was selected for the adsorption isotherm to ensure equilibruim state is achieved.

In batch setup, adsorption isotherms of Sc with BP-TCPSi and TCPSi particles were performed with initial concentrations of Sc corresponding to 0.1 – 2.5 mg/L at pH 1 and 0.1 – 4 mg/L at pH 3. In case of Dowex 50WX8, the concentrations were 2 – 45 mg/L at pH 1 and 2 – 65 mg/L at pH 3. Langmuir equations were fitted to the experimental isotherm datasets (Figure 4), and the parameters from the fittings are listed in Table 2.
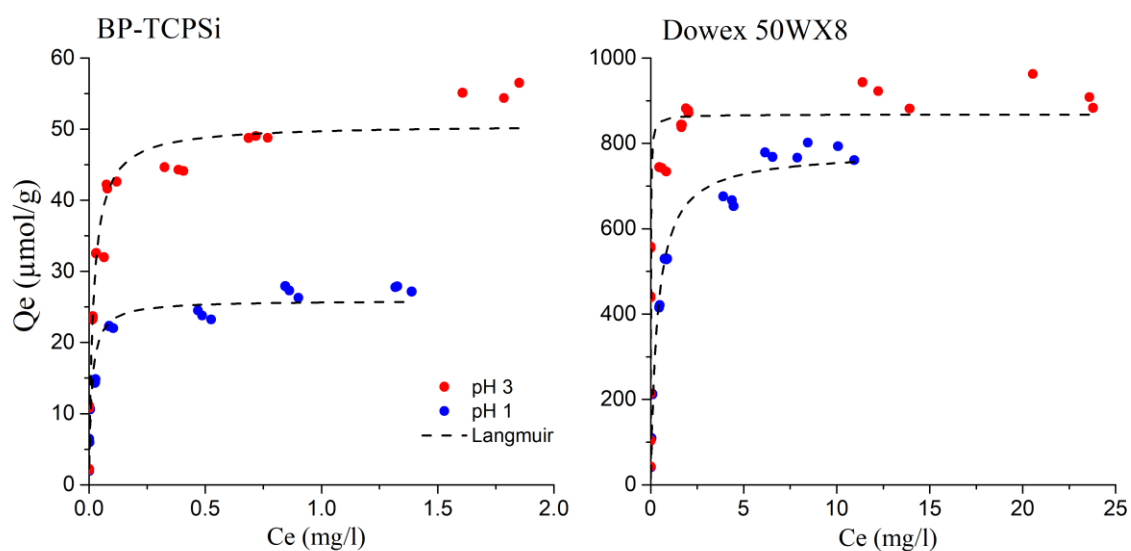
Figure 4. Adsorption isotherms of Sc with BP-TCPSi particles and Dowex 50WX8 resin at pH 1 and pH 3.

Table 2. Results of Langmuir isotherm parameters. Qmax is the maximum capacity and K_L is Langmuir constant.

Sample		Langmuir		
		Qmax (µmol/g)	K_L (L/mg)	R^2
BP-TCPSi	pH 1	26 ± 1	84 ± 14	0.94
	pH 3	51 ± 1	53 ± 8	0.95
Dowex 50WX8	pH 1	781 ± 14	2.7 ± 0.2	0.98
	pH 3	868 ± 34	93 ± 20	0.86

Unfunctionalized TCPSi particles adsorbed a negligible amount of Sc at pH 1 (3.1 ± 1.0 µmol/g) and at pH 3 (5.1 ± 1.5 µmol/g) (Figure S6). Since there were no active metal binding sites in TCPSi, the adsorption can be attributed to electrostatic interaction or physisorption, and the experimental data did not fit to the Langmuir model. In case of BP-TCPSi and Dowex 50WX8, the goodness of the Langmuir fit was given by the nonlinear regression coefficient R^2 values. The values were greater than 0.86 indicating that the adsorption follows the Langmuir model in all cases. This means that specific interaction between the metal ion and adsorption

site exists. The main ligands for the adsorption sites are phosphoric acid groups in the BP-TCPSi particles and sulfonic acid groups in the Dowex 50WX8 resin.

Maximum capacity (Qmax) of BP-TCPSi at pH 1 was two times lower than at pH 3. The isotherm results can be explained by the proton exchange mechanism from the phosphonate groups, where the first deprotonation ($pKa_1 = 1$) occurs at pH 1 and second ($pKa_2 = 2.5$) at pH 3. The OH group connected to the geminal C-atom only deprotonates in very high pH value (pH > 9) [22] and therefore do not have any contribution in the adsorption in the studied pH range alike the 3rd and 4th deprotonations. Another adsorption mechanism of Sc ion is related to the formation of coordination bond with P=O group by virtue of the lone pair of electrons in the O-atom.[21,23] Therefore, chelation occurs by the synergy of the proton exchange mechanism alongside the formation of coordinate bond with P=O.[23] In stoichiometric terms, the obtained Qmax value did not exceed the BP grafted on the particles, 59 μmol/g, implying also that the adsorption was mainly chemisorption.

Oxidation state of Sc in aqueous solution is Sc (III). It can be hypothesized that because of a single deprotonation at pH 1 inducing only one anionic O-atom per BP molecule (monodentate ligand), multiple BP molecules participated in capture of a single Sc cation yielding a low Qmax value at saturation. On the contrary, at pH 3, bidentate BP ligands with two deprotonated O-atoms yielded higher adsorption. It should be noted from Figure 3 that the Sc adsorption with the BP-TCPSi at pH 3 did not saturate completely meaning that there are possibly another binding mechanism beside the Langmuir model. Isoelectric point of unfunctionalized TCPSi is pH 2.6.[24] This means unconjugated carbon surfaces in BP-TCPSi at pH 3 enhanced the adsorption via electrostatic interaction as in the case with TCPSi particles where the adsorption followed almost linear model. Nonetheless, the adsorption capacity of BP-TCPSi was considerably lower than the commercial Dowex 50WX8 resin by 30 fold at pH 1 and 15 fold at pH 3.

For comparison to a previous study[13], Qmax of Sc at pH 3 with bare mesoporous silica materials; silica gel, KIT-6 and SBA-15 were 12, 22 and 25 μmol/g respectively despite of exceptionally high surface areas (378, 850 and 934 m^2/g) , pore volumes (0.9, 1.1 and 1.2 cm^3/g) and pore diameters (15, 7.7 and 7.6 nm).[13] In addition, there was virtually no Sc adsorbed with KIT-6 at lower pH (1.6 – 1.9) due to strong electrostatic repulsion between the metal ion and silica surfaces.[13] The results of present study therefore emphasizes the significance of surface modification with suitable metal chelating moieties to complement metal adsorption properties of the mesoporous materials.

3.2.2 Flow-through setup

Unlike batch type, the centrifugation step was not required in flow-through setup. Here, the feed solution was continuously flown through the adsorbent with the flow-rates and volumes as described above. This setup was employed to examine i) the selectivity of BP-TCPSi and Dowex 50WX8 towards Sc and b) the reusability of BP-TCPSi upto 50 adsorption/desorption cycles of Sc.

3.2.2.1 Scandium selectivity

Selectivity of BP-TCPSi and Dowex 50WX8 towards Sc was surveyed in an equimolar mixture of Sc^{+3}, Al^{+3}, Fe^{+3}, Cu^{+2} and Zn^{+2} with initial amount of each metal corresponding to 1:1 molar ratio to the maximum capacity for Sc. Therefore, with the BP-TCPSi, initial concentrations of every metal were adjusted to 110 µmol/L (pH 1) and 220 µmol/L (pH 3). In case of the Dowex 50WX8 resin, the equimolar concentration was 3100 µmol/L (pH 1) and 3300 µmol/L (pH 3). The results with Dowex 50WX8 resin at pH 3 was unreliable due to precipitation of Fe^{3+} and thus discarded to avoid false interpretation. To provide distinct comparison of the selectivity between the adsorbents and pH values, a separation factor (SF) was calculated using following equation.

$$SF = \frac{C_{des(Sc)}}{C_{des(Al+Fe+Cu+Zn)}} \bigg/ \frac{C_{0(Sc)}}{C_{0(Al+Fe+Cu+Zn)}} \quad (3)$$

The calculated SF value quantified how effectively Sc was purified from the original metal mixture after a complete adsorption/desorption cycle, which is a crucial measure of the adsorbent's efficacy. The selectivity results are shown in Figure 5.
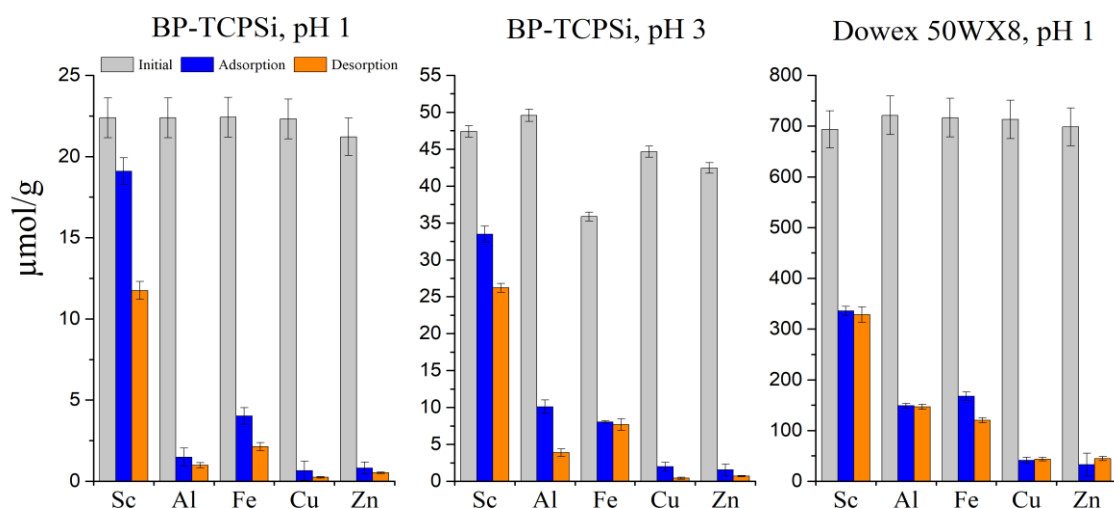

Figure 5. Metal selectivity results of BP-TCPSi and Dowex 50WX8 at pH 1 and pH 3. Error bars represent SD (n=3).

Sc selectivity with BP-TCPSi was preferable at pH 1 (SF = 13 ±1) than at pH 3 (SF = 8 ± 1). Compared to Dowex 50WX8 (SF = 4.3 ± 0.2), BP-TCPSi was 3-fold superior to selectively extract Sc when the adsorption was conducted at pH 1. The sum of all adsorbed metal amounts in BP-TCPSi were 26 ± 3 µmol/g (pH 1) and 55 ± 3 µmol/g (pH 3) and in Dowex 50WX8 was 726 ± 41 µmol/g (pH 1) corresponding to the Qmax values listed in Table 2. This means that the active binding sites in the adsorbents were fully occupied while unspecific adsorption was prohibited. Based on eqn (3), the SF value is directly proportional to the desorption efficiency. It should be noted that the desorption of Sc from the BP-TCPSi particles was not 100 %, which abated higher SF values.

As a generic rule, adsorption is directly proportional to ionic charge thus; divalent Cu^{2+} and Zn^{2+} had the least adsorption efficiencies and were incompetent amongst the other metals for selective adsorption. Competitive adsorption of Sc^{3+} with Al^{3+} and Fe^{3+} was expected, as they

9

are all trivalent cations and possess analogous chemical properties relating to Lewis acidity and similar atomic size. [6,20,21]. Presented results clearly displayed higher selectivity for Sc^{3+} than other metals in the solution, substantially with BP-TCPSi and moderately with Dowex 50WX8.

The observed selectivity can be related to the Eisenman model of selectivity.[25] This model postulated that less hydrated ions are more likely to be specifically adsorbed, since dehydration can occur easier.[26] Hydration enthalpy is then related to the ionic potential of a metal. Depending upon the ionic potential, water molecules bound to the metal ion. Ionic radius of Sc^{3+}, Al^{3+} and Fe^{3+} are respectively 0.0885, 0.0785 and 0.0675 nm. Sc^{3+} with largest ionic radius have the least ionic potential. Hence, the hydration energies as in the order Sc (-3897 KJ/mol) < Fe (-4430 KJ/mol) < Al (-4665 KJ/mol)[27] are logical to explain the observed selectivity.

The higher selectivity of BP-TCPSi towards Sc at pH 1 compared to pH 3 can be related to the difference in binding affinities given by the Langmuir constant (K_L) values (see Table 2) such that K_L (pH 1) > K_L (pH 3). Further, the type of reaction involved in the binding as briefly investigated by isotherm titration calorimetric (ITC) analysis revealed exothermic reaction (-ve ΔH) at pH 1 but endothermic (+ve ΔH) at pH 3 (Figure S13). This implies that the binding was spontaneous at pH 1 (enthalpy driven) but non-spontaneous or entropy driven at pH 3. The exothermic reaction at pH 1 affirmed formation of stronger Sc complexes and therefore not easily reversible.

Despite distinctive characteristics between the BP-TCPSi particles and the Dowex 50WX8 resin, functional moieties (the ligands and its denticity) in the adsorbent determine the adsorption properties. Higher Sc selectivity observed with the BP-TCPSi particles compared to the Dowex 50 WX8 can be explained by the metal-ligand bite angles. Ligands with larger bite angle favors larger ions while the smaller bite angle to smaller ions. [28,29] The O-Sc-O angle in the $Sc-PO_4$ complexes have wider and larger range of 63.35 – 104.76° than in the $Sc-SO_4$ complexes of 82.96 – 95.61°.[29]

3.2.2.2 Reusability of BP-TCPSi

Because of the superior Sc selectivity obtained at pH 1, reusability of the BP-TCPSi was investigated using Sc solution (5 mg/L) also at pH 1 for the adsorption. Consecutive 50 adsorption/desorption cycles were completed and the results are shown in Figure 6.
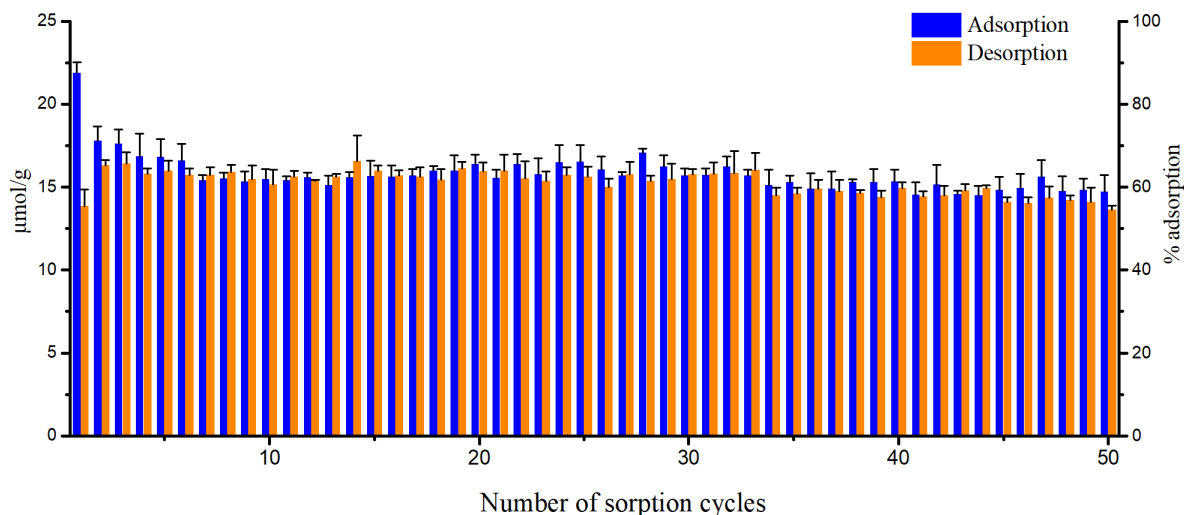
Figure 6. Reusability of BP-PSi for 50 adsorption/desorption cycles of Sc. Error bars represent SD (n=4).

In the 1st cycle, adsorption was 84 ± 2 % of Qmax, out of which 21 ± 4 % Sc remained in the particles because only 63 ± 5 % of the adsorbed amount was desorbed. It is proclaimed also in literature that the Sc ions being Pearson hard acids prefers to form strong complexes with phosphate groups and is therefore difficult to be desorbed by inorganic acids.[6,29,30] Nevertheless, the reusability results demonstrated steady adsorption and desorption from the 2nd to 50th cycle in all consecutive cycles; with an average of 60 ± 4 % adsorption and 98 ± 4 % desorption. The average TGA mass loss of BP-TCPSi measured after the 50 cycles was 2.3 ± 0.6 % w/w, which was 0.3 % w/w higher compared to untreated BP-TCPSi (Figure S11). The increase in mass loss is because of the dissolution of unreacted silicon framework under carbide layer. Crucially, there was no reduction in the mass loss confirming that BP molecules were conjugated with extreme stability in the particles withstanding 50 adsorption/desorption cycles. In addition, there was no compelling difference in the structure and morphology between the untreated BP-TCPSi and cycled BP-TCPSi by visual inspection of SEM images (Figure S12).

4. Conclusions

Bisphosphonate molecules directly grafted on carbonized surfaces of mesoporous silicon; the BP-TCPSi particles provided efficient selectivity and robust stability to adsorb scandium. The adsorption followed Langmuir isotherm model and revealed a pH dependent phenomenon. An easy-to-use filtration system was demonstrated to utilize the particles as filters for the scandium extraction. With a continuous flow of an equimolar metal mixture at pH 1, the separation factor of the BP-TCPSi particles towards scandium was 3-fold higher than that of a commercialized ion exchange resin Dowex 50WX8. A major shortcoming of the BP-TCPSi is its relatively low adsorption capacity. However, the hybrid material withstood 50 adsorption-desorption cycles without reduction in the performance. The BP-TCPSi adsorbent exhibited the fundamental requirements; the selectivity and the reusability to extract scandium. Hence, the hybrid material together with the filtration system have a great potential be employed in an industrial scale to efficiently produce scandium in an environmentally friendly manner.

References

1. Ahmad Z. The properties and application of scandium-reinforced aluminum. *JOM*. 2003;55(2):35-39. https://search.proquest.com/docview/232577616. doi: 10.1007/s11837-003-0224-6.

2. Badwal SPS, Ciacchi FT, Milosevic D. Scandia–zirconia electrolytes for intermediate temperature solid oxide fuel cell operation. *Solid State Ionics*. 2000;136(1-2):91-99. https://www.sciencedirect.com/science/article/pii/S0167273800003568. doi: 10.1016/S0167-2738(00)00356-8.

3. Akiyama M, Kamohara T, Kano K, Teshigahara A, Takeuchi Y, Kawahara N. Enhancement of piezoelectric response in scandium aluminum nitride alloy thin films prepared by dual reactive cosputtering. *Advanced materials (Deerfield Beach, Fla.)*. 2009;21(5):593-596. https://www.ncbi.nlm.nih.gov/pubmed/21161988. doi: 10.1002/adma.200802611.

4. Gambogi J, U.S. Geological Survey. Mineral commodity summaries. *Mineral commodity summaries*. 2019.

5. Wang W, Pranolo Y, Cheng CY. Metallurgical processes for scandium recovery from various resources: A review. *Hydrometallurgy*. 2011;108(1):100-108. https://www.sciencedirect.com/science/article/pii/S0304386X11000648. doi: 10.1016/j.hydromet.2011.03.001.

6. Wang W, Cheng CY. Separation and purification of scandium by solvent extraction and related technologies: A review. *Journal of Chemical Technology & Biotechnology*. 2011;86(10):1237-1246. https://onlinelibrary.wiley.com/doi/abs/10.1002/jctb.2655. doi: 10.1002/jctb.2655.

7. Na Zhang Hong-Xu Li Xiao-Ming Liu. Recovery of scandium from bauxite residue-red mud：a review. *Rare Met*. 2016;35(12):887-900. http://lib.cqvip.com/qk/85314X/201612/670906071.html. doi: 10.1007/s12598-016-0805-5.

8. Florek J, Giret S, Juère E, Larivière D, Kleitz F. Functionalization of mesoporous materials for lanthanide and actinide extraction. *Dalton transactions (Cambridge, England : 2003)*. 2016;45(38):14832-14854. https://www.ncbi.nlm.nih.gov/pubmed/27240525. doi: 10.1039/c6dt00474a.

9. Hérès X, Blet V, Di Natale P, et al. Selective extraction of rare earth elements from phosphoric acid by ion exchange resins. *Metals*. 2018;8(9):682. https://www.openaire.eu/search/publication?articleId=dedup_wf_001::fc295667fde2caa1d96b8da45dca248a. doi: 10.3390/met8090682.

10. Pugh KC, York EJ, Stewart JM. Effects of resin swelling and substitution on solid phase synthesis. *International journal of peptide and protein research*. 1992;40(3-4):208-213. https://www.ncbi.nlm.nih.gov/pubmed/1478778. doi: 10.1111/j.1399-3011.1992.tb00293.x.

11. Stability of mesoporous silica under acidic conditions. Www.rsc.org/advances PAPER. . . doi: 10.1039/c2ra21569a.

12. Florek J, Chalifour F, Bilodeau F, Larivière D, Kleitz F. Nanostructured hybrid materials for the selective recovery and enrichment of rare earth elements. *Advanced Functional Materials*. 2014;24(18):2668-2676. https://onlinelibrary.wiley.com/doi/abs/10.1002/adfm.201303602. doi: 10.1002/adfm.201303602.

13. Simon Giret, Yimu Hu, Nima Masoumifard, et al. Selective separation and pre-concentration of scandium with mesoporous silica. . . doi: 10.1021/acsami.7b13336.

14. Zhang L, Chang X, Zhai Y, et al. Selective solid phase extraction of trace sc(III) from environmental samples using silica gel modified with 4-(2-morinyldiazenyl)- N-(3-(trimethylsilyl)propyl)benzamide. *Analytica Chimica Acta*. 2008;629(1):84-91. https://www.sciencedirect.com/science/article/pii/S0003267008016607. doi: 10.1016/j.aca.2008.09.039.

15. Tu Z, Hu Z, Chang X, et al. Silica gel modified with 1-(2-aminoethyl)-3-phenylurea for selective solid-phase extraction and preconcentration of sc(III) from environmental samples. *Talanta*. 2010;80(3):1205-1209. https://www.sciencedirect.com/science/article/pii/S0039914009006985. doi: 10.1016/j.talanta.2009.09.009.

16. Hu Y, Drouin E, Larivière D, Kleitz F, Fontaine F. Highly efficient and selective recovery of rare earth elements using mesoporous silica functionalized by preorganized chelating ligands. *ACS applied materials & interfaces*. 2017;9(44):38584-38593. https://www.ncbi.nlm.nih.gov/pubmed/28968062. doi: 10.1021/acsami.7b12589.

17. Royal Society of Chemistry (Great Britain). RSC advances. .

18. Petri A Turhanen, Jouko J Vepsäläinen, Sirpa Peräniemi. Advanced material and approach for metal ions removal from aqueous solutions. *Scientific reports*. 2015;5(1):8992. https://www.ncbi.nlm.nih.gov/pubmed/25758924. doi: 10.1038/srep08992.

19. Alanne A, Hyvönen H, Lahtinen M, et al. Systematic study of physicochemical properties of a homologous series of aminobisphosphonates. . 2012. https://www.openaire.eu/search/publication?articleId=od_____1222::62f6578cc5865e76ceae85e5d7b435dc.

20. Zhang W, Koivula R, Wiikinkoski E, et al. Efficient and selective recovery of trace scandium by inorganic titanium phosphate ion-exchangers from leachates of waste bauxite residue. *ACS Sustainable Chemistry & Engineering*. 2017;5(4):3103-3114. doi: 10.1021/acssuschemeng.6b02870.

21. Joris Roosen, Stijn Van Roosendael, Chenna Rao Borra, Tom Van Gerven, Steven Mullens, Koen Binnemans.*Green Chemistry*. 2016;18.2005.

22. Matczak Jon and Adravinska VV. Supramolecular chemistry and complexation abilities of diphosphonic acid. Coordination chemistry reviews 249 (2005) 2458-2488

23. Korovin V, Sc extraction recovery mechanism from P containing extractant, 2011.

24. Mäkilä E, Bimbo LM, Kaasalainen M, et al. Amine modification of thermally carbonized porous silicon with silane coupling chemistry. *Langmuir : the ACS journal of surfaces and colloids*. 2012;28(39):14045-14054. https://www.ncbi.nlm.nih.gov/pubmed/22967052. doi: 10.1021/la303091k.

25. Dzenita Avdibegovic, Wenzhong Zhang, Junhua Xu, Mercedes Regadio, Risto Koivula, Koen Binnemans. *Separation and purification technology*. 2019; (215), 81-90.

26. Teppen BJ, Miller DM. Hydration energy determines isovalent cation exchange selectivity by clay minerals. *Soil Science Society of America Journal*. 2005;70(1):31. http://soil.scijournals.org/cgi/content/abstract/70/1/31. doi: 10.2136/sssaj2004.0212.

27. Hamilton, New Zealand. University of waikato ionic hydration enthalpies. .

28. Florek J, Mushtaq A, Larivière D, Cantin G, Fontaine F, Kleitz F. Selective recovery of rare earth elements using chelating ligands grafted on mesoporous surfaces. *RSC Advances*. 2015;5(126):103782-103789. https://www.openaire.eu/search/publication?articleId=od_____3751::805427dc2a24d9e6ce3d1e585cb83a24. doi: 10.1039/C5RA21027E.

29. Sears JM, Boyle TJ. Structural properties of scandium inorganic salts. *Coordination Chemistry Reviews*. 2017;340(C):154-171. https://www.sciencedirect.com/science/article/pii/S0010854516304441. doi: 10.1016/j.ccr.2016.12.005.

30. Pyrzyńska K, Kilian K, Pęgier M. Separation and purification of scandium: From industry to medicine. *Separation & Purification Reviews*. 2019;48(1):65-77. http://www.tandfonline.com/doi/abs/10.1080/15422119.2018.1430589. doi: 10.1080/15422119.2018.1430589.
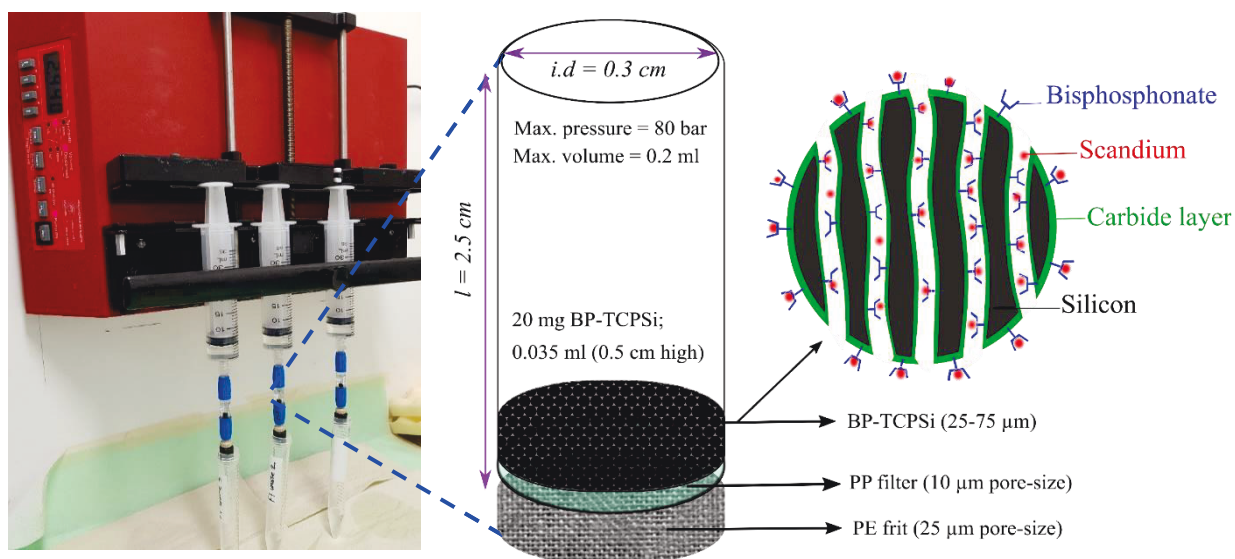
Supplementary Information

Figure S1. Schematic diagram of the lab scale flow-through setup employed in this study.
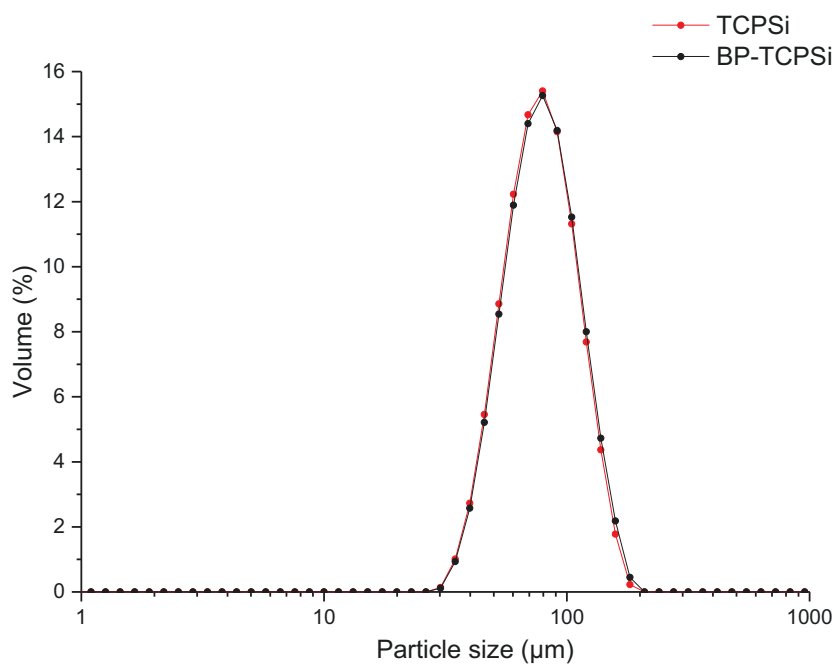

Figure S2. Particle size volume distribution of TCPSi and BP-TCPSi samples measured by Mastersizer device. Corresponding median size of the particles were 72.3 and 73.3 μm.
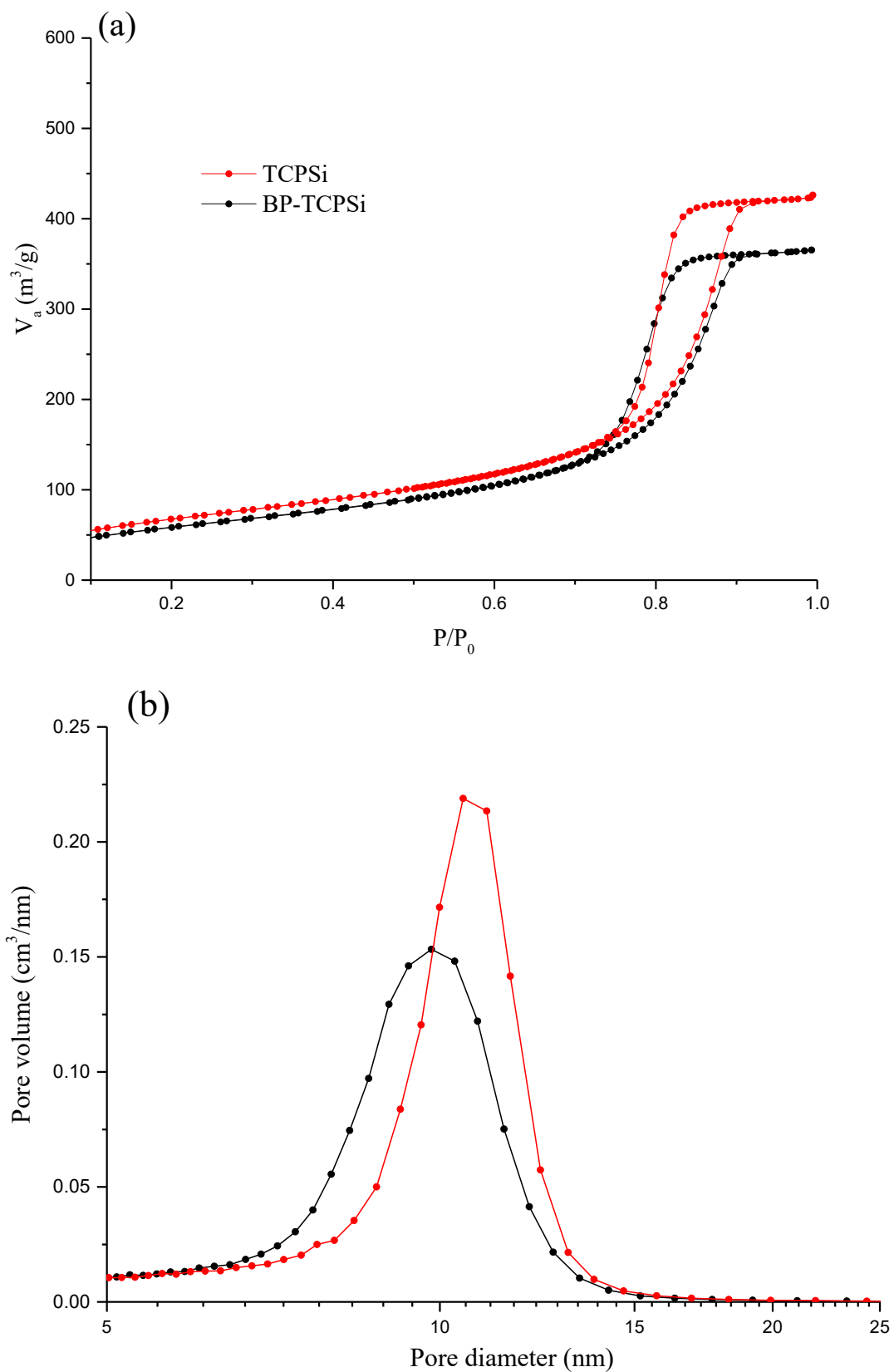
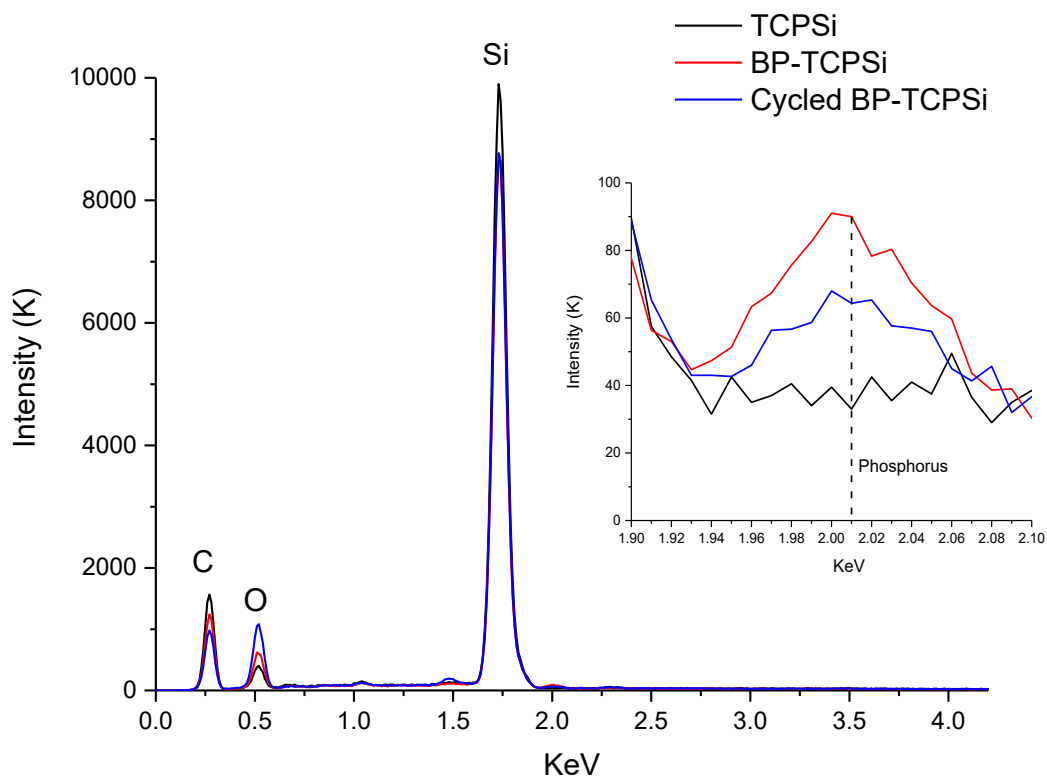Figure S3. N$_2$ physisorption isotherms (a) and pore size distribution (b) of TCPSi and BP-TCPSi samples.

Figure S4. EDS spectra of the samples; TCPSi, BP-TCPSi and cycled BP-TCPSi after 50 adsorption/desorption stages. A small peak of Phosphorous (P) at KeV 2.01 was observed in BP functionalized particles.
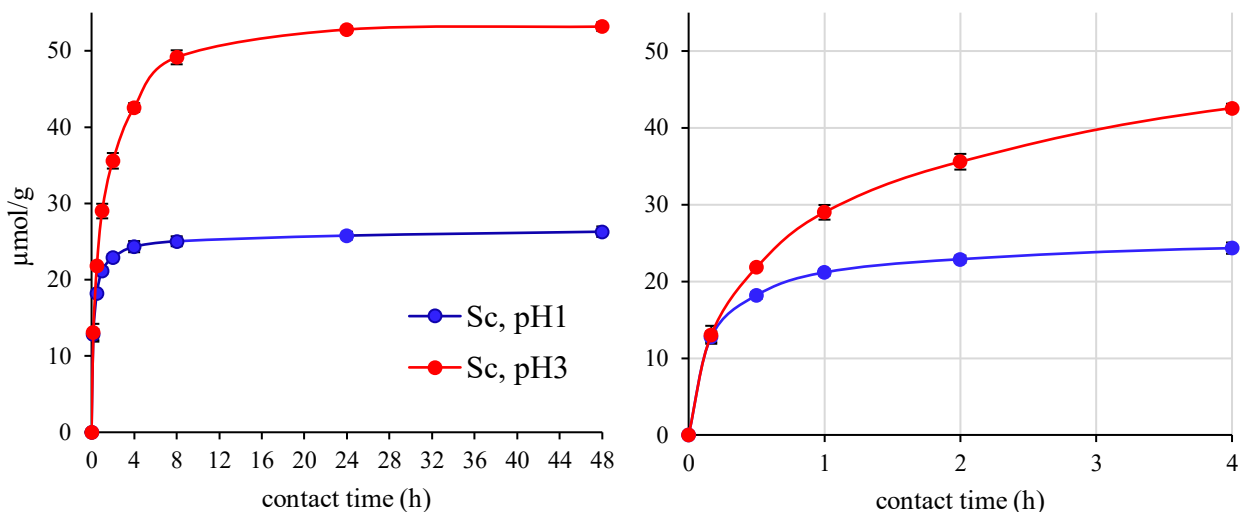
Figure S5. Adsorption kinetics of Sc with BP-TCPSi at pH 1 and pH 3. Error bars represent SD (n=3). Experimental conditions: 10 mg BP-TCPSi, V = 10 mL, C_0 = 1.5 mg/L (pH 1) and 2.5 mg/L (pH 3).
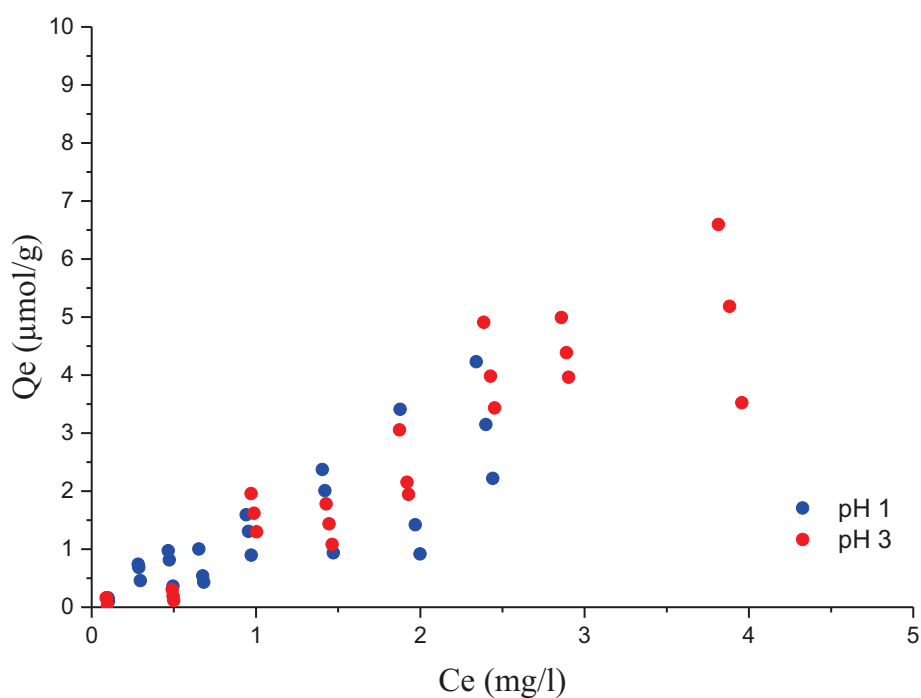
Figure S6. Adsorption isotherms of Sc with TCPSi particles at pH 1 and pH 3.
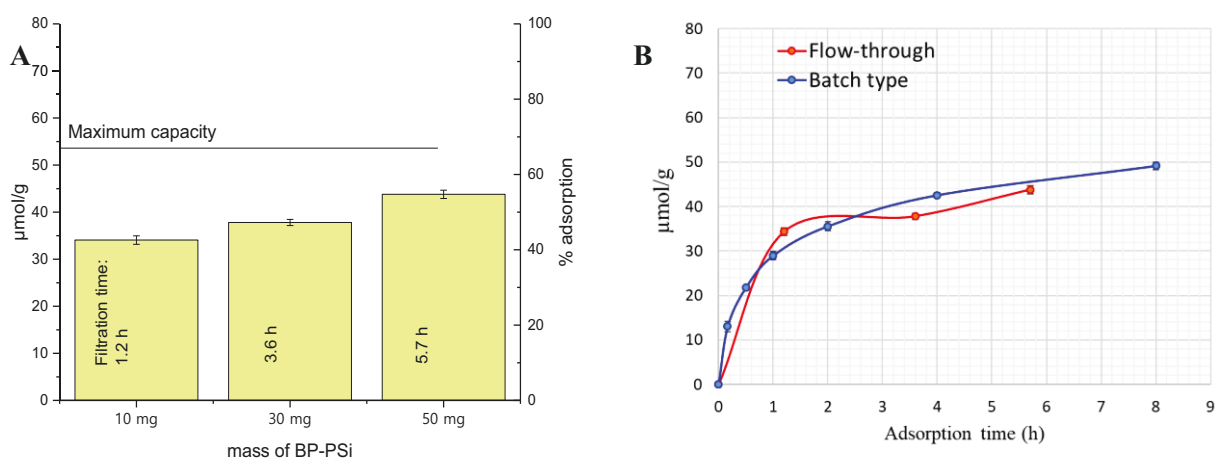
Figure S7. Effect of BP-TCPSi mass (bed volume) on Sc adsorption in flow-through setup. (A). Adsorption: 5 mg/L Sc at pH 3. Ads. vol. were respectively 7, 21, and 36 ml corresponding to $1.5 \times$ Qmax of BP-TCPSi. Flow-rate; 0.1 ml/min. Error bars represent SD (n=3). The filtrations were repeatable/suitable even with 10 mg adsorbent bed with SD below 0.9 in between the replicates. The adsorption amounts corresponded to batch type adsorption kinetics results (B).
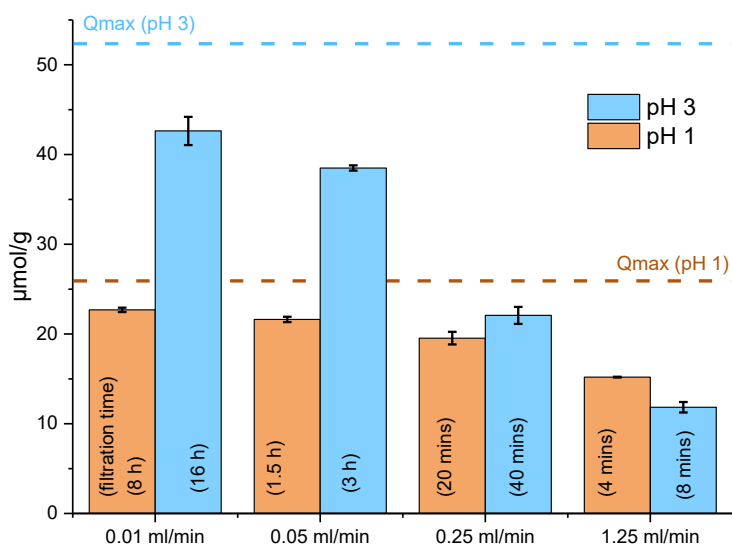
Figure S8. Effect of flow-rate on Sc adsorption with BP-PSi. Experimental conditions; 5 mg/L Sc, adsorption volumes 4.68 ml (pH 1) and 9.53 ml (pH 3). At both pH conditions, effect of flow-rate was significant (p value < α; 0.5). The F values were 205 (pH 1) and 648 (pH 3) at F critical value of 4; effect of flow-rate was 3 fold more significant at pH 3 than at pH 1. These results are in agreement with the batch type adsorption kinetics results where rate of Sc adsorption had disparity between the pH values.
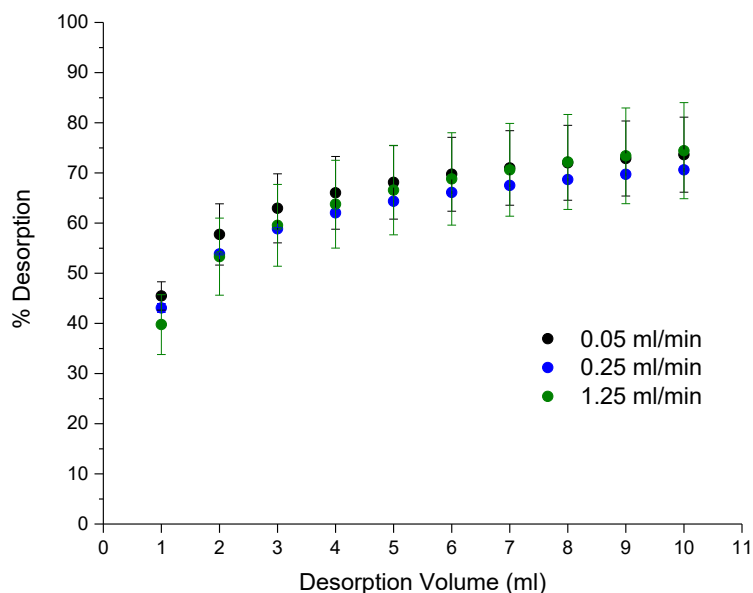

Figure S9. Effect of flow rate on Sc desorption. Experimental parameters: 20 mg BP-TCPSi, adsorption; 10 ml of 5 mg/L Sc at pH 1 at 0.5 ml/min (20 minutes), desorption; 10 ml of 1 M HNO_3. With all tested flow-rates, over 50% of the desorbed Sc was collected within 1 ml of acid flown through the BP-TCPSi. As the desorption was instantaneous, it is possible to enrich Sc extraction. The effect of flow-rate in desorption was not significant at α=0.05 with p-value 0.13 > α and F value (2.5) < F critical value (4).
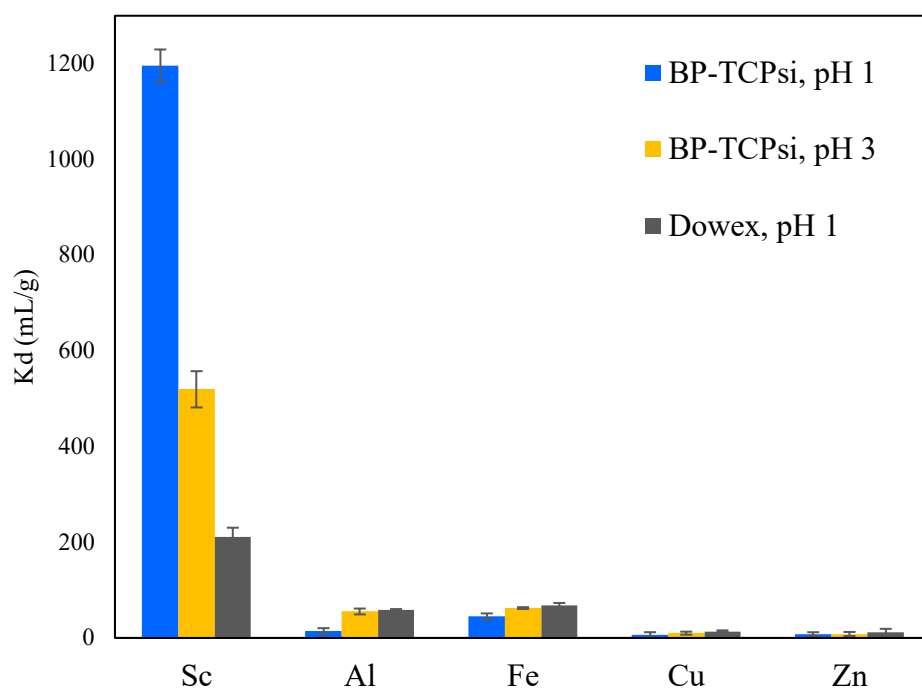
Figure S10. Distribution coefficient (K_d) values calculated from the selectivity results. The K_d value is calculated as $(C_0-C_e)/C_e * (V/m)$.
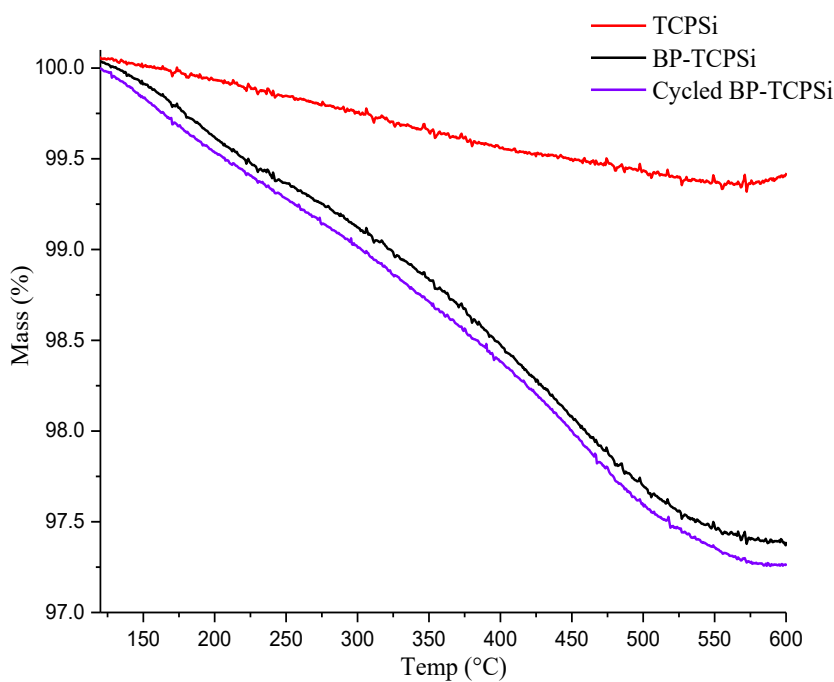

Figure S11. TGA curves of TCPSi, BP-TCPSi and cycled BP-TCPSi (50 adsorption/desorption tests).
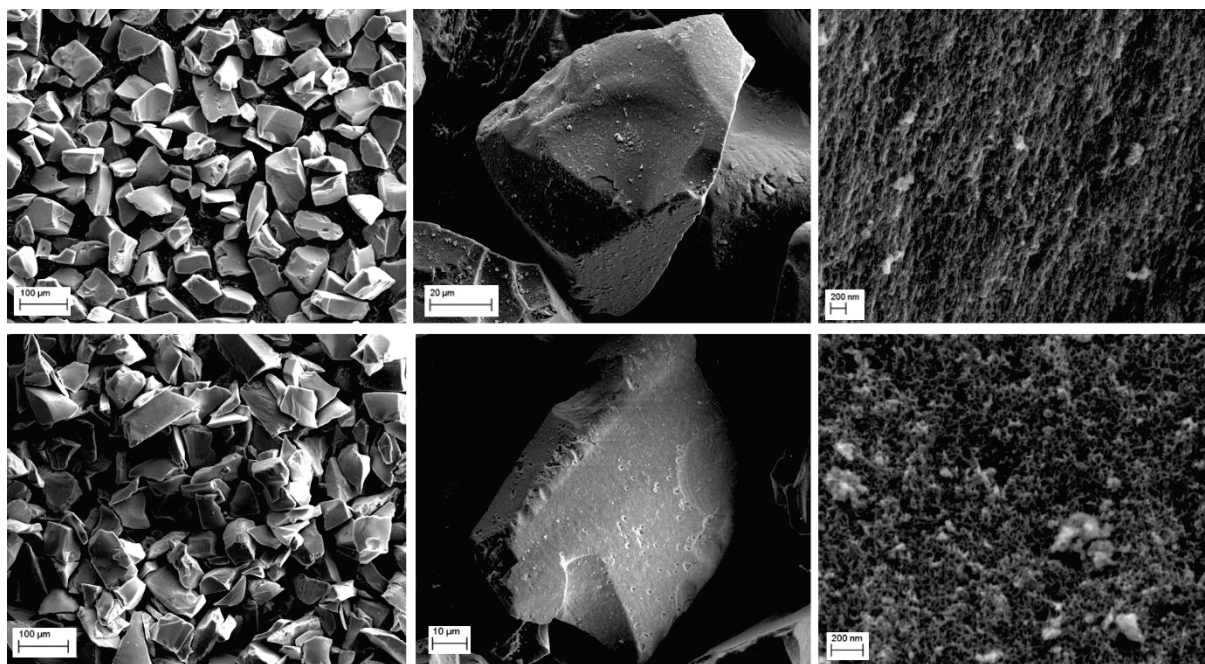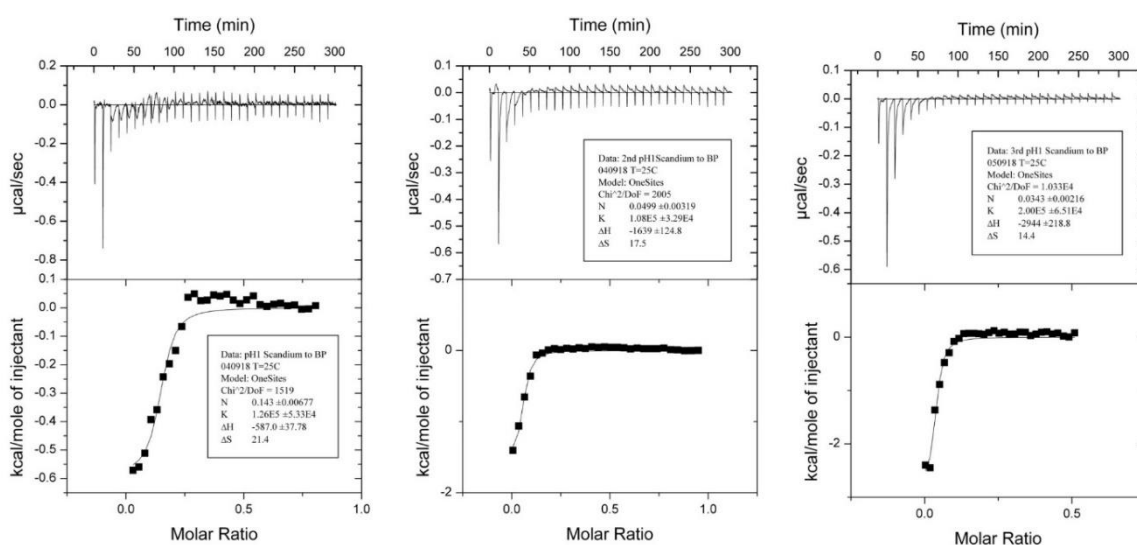
Figure S12. SEM images of TCPSi (upper three) and cycled BP-TCPSi (below three).
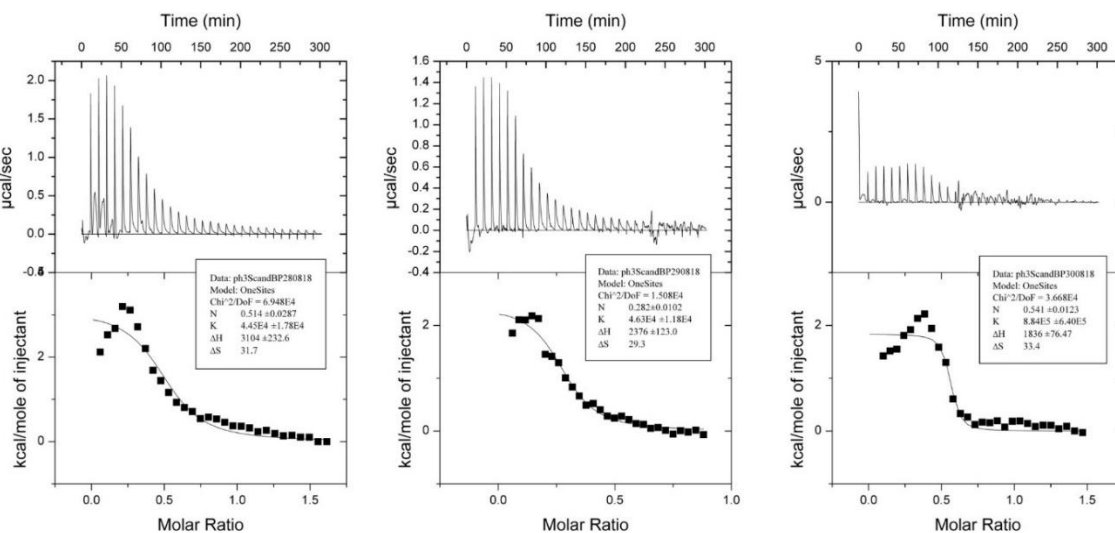
pH1

pH3

Figure S13. Results of isotherm titration calorimetric (ITC) analysis for Sc adsorption with BP-TCPSi at pH 1 and pH 3. The binding reaction was exothermic at pH 1 but endothermic at pH 3. Three individual measurements was done at each pH value. The thermodynamic equilibrium constant, K values were greater at pH 1 than at pH 3 (except the 3rd measurement). The erroneous results is due to the uncertainty in BP concentration as the particles were ground into ≤10 µm fraction in order to successfully inject the particles into the device (VP-ITC Malvern, Microbial Inc.). The measurement protocol is briefly described below.

The particles were re-dispersed in pH water (pH 1 or pH 3) and degassed prior to the measurements. The BP-TCPSi suspension; 0.9 – 1.14 mM at pH1 and 0.57 – 1.0 mM at pH3 respectively were placed into the ITC cell and titrated with 4.0 mM Sc that was placed to the syringe. The heat evolved or consumed in each titration of 10 µl injections were measured at 25 °C under constant 440 rpm stirring. Reference measurements buffer-to-buffer, buffer-to-particles and scandium-to-buffer were subtracted from the actual binding measurement.